Facile One-Pot Synthesis of PbSe and $NiSe_2$ Hollow Spheres: Kirkendall-Effect-Induced Growth and Related Properties

Genqiang Zhang,[†] Wei Wang,[†] Qingxuan Yu,[†] and Xiaoguang Li*[,†,‡]

Hefei National Laboratory for Physical Sciences at Microscale, Department of Physics, University of Science and Technology of China, Hefei, 230026, P. R. China, and International Center for Materials Physics, Academia Sinica, Shenyang 110015, P. R. China

Received September 6, 2008. Revised Manuscript Received January 19, 2009

A facile one-pot polyol process for the synthesis of PbSe and $NiSe_2$ hollow spheres, using α-Se solid spheres as starting core materials was successfully developed. The careful characterization of the time-dependent products demonstrates that the Kirkendall effect could be the involved growth mechanism for the evolution process from Se solid spheres to PbSe and $NiSe_2$ hollow spheres, which is schematically illustrated as a two-stage temperature-controlled, Kirkendall-effect-directed formation. The microstructure analysis shows that both the PbSe and $NiSe_2$ hollow spheres are polycrystalline with cubic structure. The band gap of the PbSe hollow spheres exhibits a notable size effect, and the magnetic susceptibility of the $NiSe_2$ hollow spheres is significantly increased compared with that of its bulk counterpart. This work indicates that the nonmetal Se solid spheres can act as an appropriate fast diffusion core material for hollow structure through Kirkendall effect in the solution phase method.

1. Introduction

Because of the affinitive relationship between the shape and property, how to control the morphology has always been one of the central subjects for nanomaterials.[1] Hollow spheres, in terms of their high surface areas and low material density, have been considered as the ideal building blocks for catalysis, nanoelectronics, and drug-delivery applications.[1,2] Therefore, much effort has been devoted to develop preparative methods for hollow spheres, and great progress has been achieved over the past decades.[3,4] The previous reports indicate that the hollow structure can be created through template-assisted strategies, direct solid evacuation with Ostwald ripening, or formed under oriented attachment and a Kirkendall-effect-induced process.[3,4] The application of the Kirkendall effect in a nanoscale system for hollow structures has particularly attracted extensive interest after its success on fabricating CoS_x and CoO hollow spheres by Alivisatos et al., for the possible generality in synthesizing hollow structures combined with reasonable procedures.[5] It is known that the most challenging factor to produce hollow spheres by the Kirkendall effect is to find a kind of faster diffusion material as spherical core followed by carefully controlling the interdiffusion process at the interfaces.[6] Until now, several metal solid particles have been found to be appropriate as the core materials for the synthesis of the related hollow structures.[7] About the use of amorphous selenium (α-Se) for hollow structures, Xia's group developed a facile route based on the galvanic replacement reaction for the synthesis of various Se@metal selenides structure or metal selenides hollow spheres, which greatly stimulated the research works on this area.[4] In this work, we applied the α-Se as a kind of nonmetal fast diffusion couple, which can well act as the core material for obtaining metal selenides hollow spheres through a facile two-stage temperature controlled one-pot polyol route based on the Kirkendall effect mechanism.

* Corresponding author. Phone: 86-551-3603408. Fax: 86-551-3603408. E-mail: lixg@ustc.edu.cn.

[†] Hefei National Laboratory for Physical Sciences at Microscale, Department of Physics, University of Science and Technology of China.

[‡] International Center for Materials Physics, Academia Sinica.

(1) (a) Alivisatos, A. P. *Science* **1996**, *271*, 933. (b) Zhang, J. Z. *Acc. Chem. Res.* **1997**, *30*, 423. (c) El-Sayed, M. A. *Acc. Chem. Res.* **2004**, *37*, 324. (d) Sargent, E. H. *Adv. Mater.* **2005**, *17*, 505. (e) Wang, X.; Zhuang, J.; Peng, Q.; Li, Y. D. *Nature* **2005**, *437*, 121. (f) Zhang, G. Q.; Lu, X. L.; Wang, W.; Li, X. G. *Chem. Mater.* **2007**, *19*, 5207.

(2) (a) Kim, S. W.; Kim, M.; Lee, W. Y.; Hyeon, T. *J. Am. Chem. Soc.* **2002**, *124*, 7642. (b) Bergbreiter, D. E. *Angew. Chem., Int. Ed.* **1999**, *38*, 28. (c) Chen, G.; Xia, D. G.; Nie, Z. R.; Wang, Z. Y.; Wang, L.; Zhang, L.; Zhang, J. J. *Chem. Mater.* **2007**, *19*, 1840.

(3) (a) Yin, Y. D.; Rioux, R. M.; Erdonmez, C. K.; Hughes, S.; Somorjai, G. A.; Alivisatos, A. P. *Science* **2004**, *304*, 711. (b) Zeng, H. C. *J. Mater. Chem.* **2006**, *16*, 649. (c) Peng, S.; Sun, S. H. *Angew. Chem., Int. Ed.* **2007**, *46*, 4155. (d) Yu, X. L.; Cao, C. B.; Zhu, H. S.; Li, Q. S.; Liu, C. L.; Gong, Q. H. *Adv. Funct. Mater.* **2007**, *17*, 1397. (e) Kim, S. J.; Ah, C. S.; Jang, D. J. *Adv. Mater.* **2007**, *19*, 1064. (f) Ying, J. Y.; Mehnert, C. P.; Wong, M. S. *Angew. Chem., Int. Ed.* **1999**, *38*, 56.

(4) (a) Jeong, U.; Xia, Y. N. *Angew. Chem., Int. Ed.* **2005**, *44*, 3909. (b) Jeong, U.; Herricks, T.; Shahar, E.; Xia, Y. N. *J. Am. Chem. Soc.* **2005**, *127*, 1098. (c) Camargo, P. H. C.; Lee, Y. H.; Jeong, U.; Zou, Z. Q.; Xia, Y. N. *Langmuir* **2007**, *23*, 2985. (d) Jeong, U.; Kim, J. U.; Xia, Y. N. *Nano Lett.* **2005**, *5*, 937. (e) Chou, N. H.; Schaak, R. E. *Chem. Mater.* **2008**, *20*, 2081. (f) Chou, N. H.; Schaak, R. E. *J. Am. Chem. Soc.* **2007**, *129*, 7339.

(5) (a) Liu, B.; Zeng, H. C. *J. Am. Chem. Soc.* **2004**, *126*, 16744. (b) Fan, H. J.; Knez, M.; Scholz, R.; Nielsch, K.; Pippel, E.; Hesse, D.; Zacharias, M.; Gösele, U. *Nat. Mater.* **2006**, *5*, 627. (c) Liang, X.; Wang, X.; Zhuang, Y.; Xu, B.; Li, Y. D. *J. Am. Chem. Soc.* **2008**, *130*, 2736.

(6) (a) Tu, K. N.; Gösele, U. *Appl. Phys. Lett.* **2005**, *86*, 093111. (b) Fan, H. J.; Knez, M.; Scholz, R.; Hesse, D.; Nielsch, K.; Zacharias, M.; Gösele, U. *Nano Lett.* **2007**, *7*, 993.

(7) (a) Nakamura, R.; Tokozakura, D.; Nakajima, H.; Lee, J. G.; Mori, H. *J. Appl. Phys.* **2007**, *101*, 074303. (b) Shao, H. F.; Qian, X. F.; Zhu, Z. K. *J. Solid State Chem.* **2005**, *178*, 3522. (c) Wang, Y.; Cai, L.; Xia, Y. *Adv. Mater.* **2005**, *17*, 473. (d) Ma, Y. W.; Huo, K. F.; Wu, Q.; Lu, Y. N.; Hu, Y. M.; Hu, Z.; Chen, Y. *J. Mater. Chem.* **2006**, *16*, 2834.

10.1021/cm803307f CCC: $40.75
Published on Web 02/11/2009

By the designed procedures, two kinds of metal selenides, PbSe and $NiSe_2$ hollow spheres with controllable diameters, are successfully fabricated. As important functional semiconductors, both PbSe and $NiSe_2$ have attracted great interest because of the potential applications in infrared detectors, selective and photovoltaic absorbers for PbSe,[8] or interesting electronic and size-dependent magnetic properties for $NiSe_2$.[9] For example, PbSe nanocrystals can be reached through an organic solvent synthesis route, solvothermal process, noble metal seed mediated route, and so on.[10] For hollow spheres of PbSe, Wang et al. reported the only concerned products till now through a complex multistep process based on reverse cation-exchange mechanism.[11] In this case, the realization of a simpler and more powerful route for controllable synthesis of PbSe hollow spheres is of great significance. For the fabrication of $NiSe_2$, the earlier reports indicated that it can be reached by a variety of methods, such as solid-state synthesis, molecular precursors, elemental direct reactions, ultrasonic synthesis, mechanical alloying, and solvothermal process.[12] However, to the best of our knowledge, it remains a challenge to develop an appropriate approach for the synthesis of $NiSe_2$ hollow spheres.

In this paper, we developed an optimized one-pot route that is appropriate for the synthesis of PbSe and $NiSe_2$ hollow spheres with controllable sizes through a low-temperature, solution-phase process based on the Kirkendall effect mechanism. The optical property of the PbSe hollow spheres and the magnetic property of the $NiSe_2$ hollow spheres are investigated.

2. Experimental Section

Lead acetate ($Pb(CH_3COO)_2 \cdot 3H_2O$), Nickel chloride ($NiCl_2 \cdot 6H_2O$), Selenium dioxide ($SeO_2$) with analytical grade were chosen as raw materials. Ethylene glycol (EG) and polyvinyl pyrrolidone (PVP, k-30, $M_s \approx 30\,000$) act as solvent and surfactant, respectively. The hydrazine ($N_2H_4 \cdot H_2O$) was selected as the reduce agent and all the synthetic processes were carried out within an oil bath at atmospheric conditions.

In a typical synthesis, 2 mmol $Pb(CH_3COO)_2 \cdot 3H_2O$ or 1 mmol $NiCl_2 \cdot 6H_2O$, 2 mmol SeO_2 powder, and an appropriate amount of PVP were dissolved into 20 mL of EG with magnetic stirring to form the corresponding precursor solution for the synthesis of PbSe and $NiSe_2$ hollow spheres. The obtained solution was transformed into a three-neck bottle followed by the addition of an excessive amount of $N_2H_4 \cdot H_2O$ into the precursor solution at about 20 °C. The solution was kept magnetically stirring for about 20 min in order to obtain α-Se products. After that, the solution was heated to 150 °C with a heating rate of 10 °C/min. The black products were collected by centrifugation after reacting for about 20 min. They were then washed with distilled water and anhydrous ethanol several times and dried in a vacuum at 60 °C for further characterization.

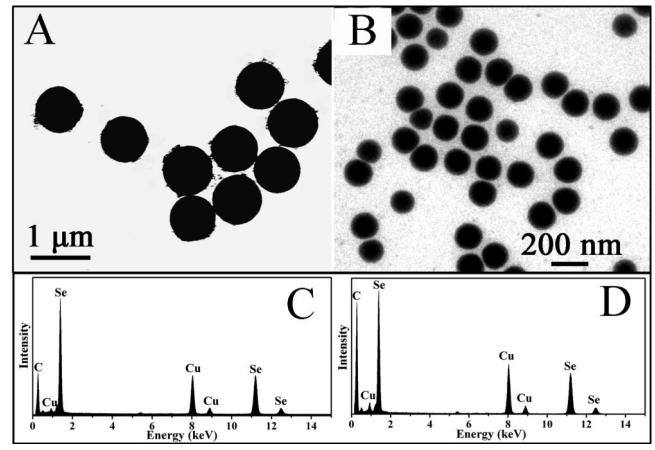

Figure 1. Typical TEM images and corresponding EDS spectra of the α-Se solid spheres obtained at 20 °C with different amounts of PVP: (A) 0 and (B) 0.6 g of PVP.

The XRD patterns of the as-prepared samples were collected on a Philips X'Pert diffractometer with Cu K*a* radiation ($\lambda = 1.5418$ Å). The products dispersed in ethanol were spread on a silicon substrate and coated with gold thin film for the FESEM measurements on a JEOL JSM-6700F scanning electron microscope. The products dispersed in ethanol were also spread on a copper grid with an organic supporting membrane for transmission electron microscopy (TEM) measurements on a Hitachi H-800 transmission electron microscope and high-resolution (HR) TEM analysis on a JEOL 2010 transmission electron microscope at an acceleration voltage of 200 kV. The optical diffuse reflectance spectra were performed on a UV−vis-NIR scanning spectrophotometer (DUV-3700, Shimdzu) using an integrating sphere accessory. The magnetization measurements were carried on a superconducting quantum interference device (SQUID) (MPMS, Quantum Design).

3. Results and Discussion

Figure 1 shows typical transmission electron microscopy (TEM) images and energy dispersive X-ray spectrum (EDS) analysis of the α-Se solid spheres obtained by reducing SeO_2 with hydrazine at 20 °C. The diameters of the Se spheres obtained with different amounts of PVP can be estimated from the TEM images (images A and B in Figure 1), which give that the diameters are about 800 nm for the products obtained with no addition of PVP and 120−140 nm for the products with 0.6 g of PVP as organic additive, respectively. The TEM images also clearly show the solid feature of the obtained α-Se spheres. The EDS spectra (panels C and D in Figure 1) further confirm the formation of the pure Se products with different diameters.

The Se solid spheres with controllable sizes obtained in this stage would act as the fast diffusion core materials for the formation of the PbSe and $NiSe_2$ hollow spheres. Figure

(8) (a) Mulik, R. N.; Rotti, C. B.; More, B. M.; Sutrave., D. S.; hahane, G. S.; Garadkar, K. M.; Deshmukh, L. P.; Hankare, P. P. *Indian J. Pure Appl. Phys.* **1996**, *34*, 903. (b) Harman, T. C.; Taylor, P. J.; Walsh, M. P.; La Forge, B. E. *Science* **2002**, *297*, 2229.
(9) (a) Sheldrick, S.; Wachhold, M. *Angew. Chem., Int. Ed.* **1997**, *39*, 206. (b) Parkin, G. *Prog. Inorg. Chem.* **1998**, *47*, 1. (c) Steigerwald, M. L.; Brus, L. E. *Acc. Chem. Res.* **1990**, *23*, 183. (d) Wang, Y.; Herron, N. *J. Phys. Chem.* **1991**, *95*, 525.
(10) (a) Murray, C. B.; Sun, S.; Gaschler, W.; Doyle, H.; Betley, T. A.; Kagan, C. R. *IBM J. Res. Dev* **2001**, *45*, 47. (b) Xu, J.; Ge, J. P.; Li, Y. D. *J. Phys. Chem. B* **2006**, *110*, 2497. (c) Shi, W. L.; Sahoo, Y.; Zeng, H.; Ding, Y.; Swihart, M. T.; Prasad, P. N. *Adv. Mater.* **2006**, *18*, 1889.
(11) Zhu, W.; Wang, W. Z.; Shi, J. L. *J. Phys. Chem. B* **2006**, *110*, 9785.
(12) (a) Bonneau, P. R.; Jarvis, R. F.; Kaner, R. B. *Nature* **1991**, *349*, 510. (b) Brennan, J. G.; Siegrist, T.; Kwon, Y. U.; Stuczynski, S. M.; Steigerwald, M. L. *J. Am. Chem. Soc.* **1992**, *114*, 10344. (c) Henshaw, I. P.; Parkin, G. A. *J. Chem. Soc., Dalton Trans.* **1997**, 231 Shaw. (d) Ge, P.; Li, Y. D. *J. Mater. Chem.* **2003**, *13*, 911. (da) Campos, C. E. M.; de Lima, J. C.; Grandi, T. A.; Machado, K. D.; Pizani, P. S.; Hinrichs, R. *Solid State Ionics* **2004**, *168*, 205. (e) Kerner, R.; Palchik, O.; Gedanken, A. *Chem. Mater.* **2001**, *13*, 1413. (f) Zhuang, Z. B.; Peng, Q.; Zhuang, J.; Wang, X.; Li, Y. D. *Chem. Eur. J.* **2006**, *12*, 211.

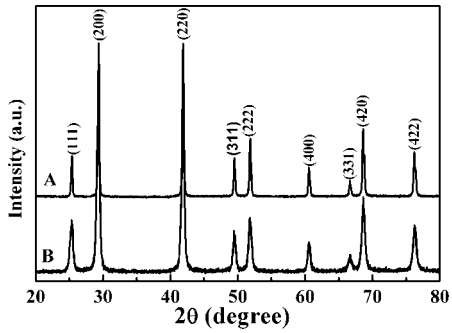

Figure 2. Typical XRD patterns of the PbSe hollow spheres obtained with different amounts of PVP after reaction at 150 °C for 20 min: (A) 0 and (B) 0.6 g of PVP.

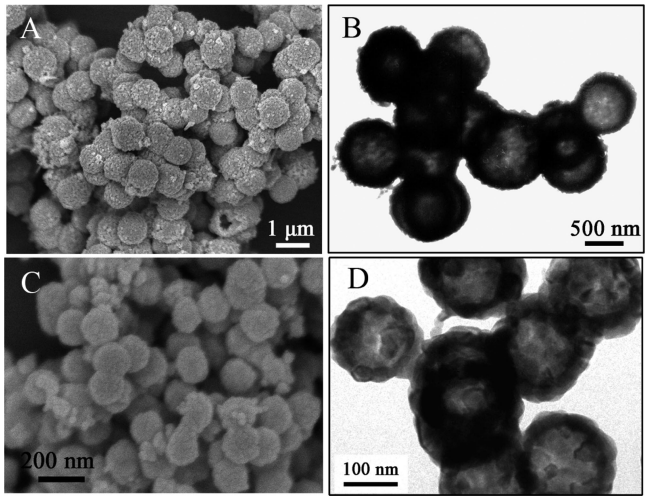

Figure 3. SEM and TEM characterizations of the PbSe hollow spheres obtained at 150 °C for 20 min with different amounts of PVP: (A, B) 0 and (C, D) 0.6 g of PVP.

2 gives the X-ray diffraction (XRD) patterns of the PbSe hollow spheres obtained with different amounts of PVP at 150 °C for 20 min. Both of these two patterns can readily be indexed as a pure cubic phase of PbSe according to the Joint Committee on Powder Diffraction Standards (JCPDS) Card 06-0354, indicating the evolution process from α-Se to crystalline PbSe hollow spheres at the elevated temperature. Corresponding to the sizes of the α-Se spheres obtained with different amounts of PVP at the low-temperature reaction stage, the diameters of the PbSe hollow spheres after reaction at 150 °C for 20 min are about 800−1000 nm (images A and B in Figure 3) and 150−180 nm (images C and D in Figure 3), respectively. The hollow character of the as-prepared PbSe hollow spheres can be confirmed by both SEM and TEM images (Figure 3), where a deep contrast along the colloid edges is clearly observed. The shell thicknesses of the hollow spheres can be estimated from the TEM images shown in images B and D in Figure 3, which are in the range of 120−150 and 20−30 nm, respectively. Further investigations of the PbSe hollow structure come from the high-resolution transmission electron microscopy (HRTEM) and EDS analyses performed on an individual PbSe hollow sphere obtained with 0.6 g PVP, as shown in Figure 4. It can be seen from Figure 4A that the PbSe hollow sphere consists of particle assembly, whose sizes range from

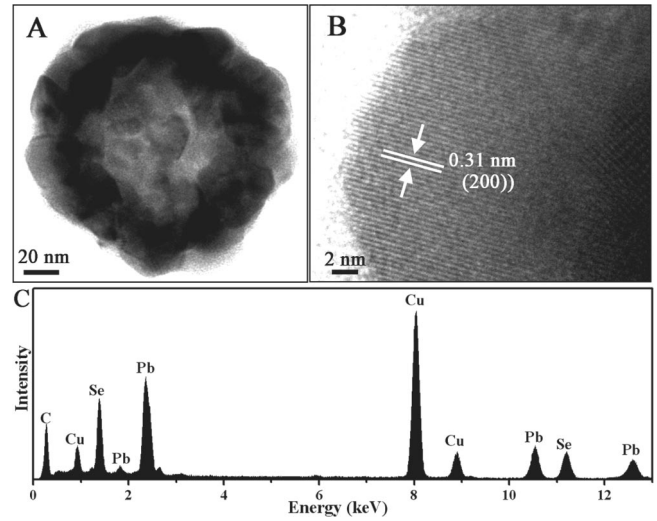

Figure 4. HRTEM analysis and EDS spectrum of the PbSe hollow spheres obtained at 150 °C for 20 min with 0.6 g of PVP: (A) TEM image of a randomly selected individual PbSe hollow sphere, (B) typical HRTEM image, and (C) EDS spectrum taken from the individual PbSe hollow sphere in (A).

10 to 20 nm. HRTEM image in Figure 4B shows clear lattice fringes, which suggest the good crystallinity of these particles. The corresponding lattice distance of about 0.31 nm matches well with that of the cubic PbSe (200) planes (0.306 nm from the JCPDS Card 06-0354), which is consistent with the XRD characterization. The composition information obtained from the EDS spectrum shown in Figure 4C gives Pb:Se molar ratio of about 1:1, which confirms the formation of PbSe compound.

To investigate the possible size effect on the band gap of the PbSe hollow spheres with different diameters, we measured their optical diffuse reflection spectra, as shown in Figure 5, where lines A and B come from the PbSe hollow spheres with diameters of about 800−1000 and 150−180 nm, respectively. It is well-known that the optical band gap (E_g) for a semiconductor can be obtained by the following equation[13]

$$\alpha(\upsilon) = A(h\upsilon/2\rho - E_g)^{m/2}$$

Where A is a constant, α is the absorption coefficient that can be obtained from the optical diffuse spectra, and m is equal to 1 for a direct allowed transition. Because α is proportional to $F(R)$, the Kubelka−Munk function, the energy intercept of a plot of $(F(R)h\upsilon)^2$ versus $h\upsilon$ yields E_g for a direct allowed transition when the linear region is extrapolated to zero ordinate. From the diffuse reflection spectra of the PbSe hollow spheres, as shown in Figure 5, the corresponding plots of $(F(R)h\upsilon)^2$ versus $h\upsilon$ can be obtained (see the insets to panels A and B in Figure 5). The band gap of the PbSe hollow spheres with different diameters of about 800−1000 and 150−180 nm are calculated to be about 0.31 and 0.67 eV, respectively. Compared with the reported value for the PbSe bulk counterpart (~0.29 eV),[14] the band gap of the as-prepared PbSe hollow spheres with diameters of 800−1000 nm is almost equal to that of the

(13) Luca, V.; Djajanti, S.; Howe, R. F. *J. Phys. Chem. B* **1998**, *102*, 10650.
(14) Streltov, E. A.; Osipovich, N. P.; Ivashkevich, L. S.; Lyakhov, A. S.; Sviridov, V. V. *Electrochim. Acta* **1998**, *43*, 869.

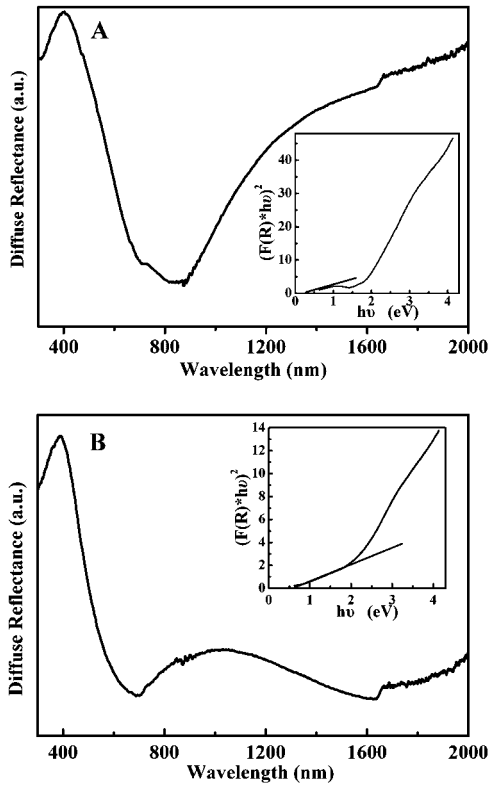

Figure 5. Room-temperature diffuse reflectance spectra of PbSe hollow spheres with different diameters: (A) 800−1000 nm, (B) 150−180 nm, and the insets is the corresponding curves plotted as $(F(R)*h\upsilon)^2$ versus $h\upsilon$ (eV).

bulk material, whereas the band gap value of the PbSe products with diameters of 150−180 nm is greatly increased. This could be derived from the particle assembly feature of the as-synthesized PbSe hollow spheres. It has been broadly proved in a semiconductor system that the reduced size can induce size quantization effects that lead to a series of discrete states in the conduction and valence bands that could greatly influence their band gaps.[15] Especially, as one of the IV−VI semiconductors, PbSe exhibits a stronger quantum confinement because of its large Bohr radius of 46 nm. In this situation, it is possible to influence the band gap of the PbSe when the particle size reaches about or even slightly larger than 10 nm.[16] In previous literatures, several reports have demonstrated the notable size effect on the band gap of the PbSe nanocrystals.[16] In our work, the PbSe hollow spheres consist of particle assembly (as shown in Figure 4A). The diameters of the small particles are in the range of 10−20 nm for the PbSe hollow spheres with diameters of

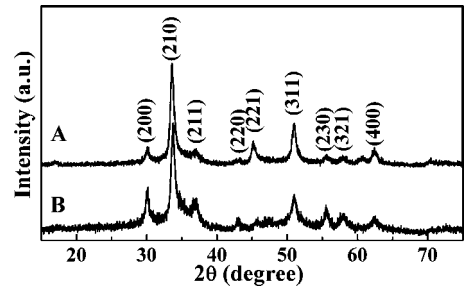

Figure 6. Typical XRD patterns of $NiSe_2$ hollow spheres obtained with different amounts of PVP: (A) 0 and (B) 0.6 g of PVP.

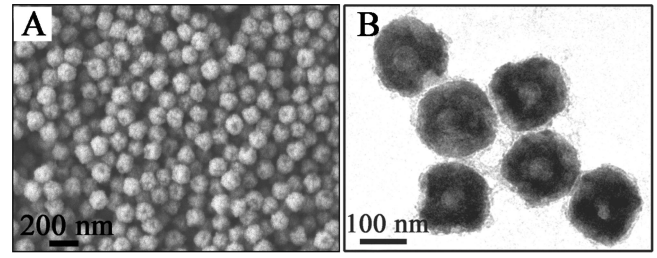

Figure 7. Morphology characterization of the $NiSe_2$ hollow spheres obtained at 150 °C for 20 min with 0.6 g of PVP: (A) SEM and (B) TEM images.

150−180 nm, which are smaller than the Bohr radius of the PbSe. This could lead to a notable effect on the electronic states and further the band gap of the PbSe hollow spheres.[16] For PbSe hollow spheres with diameters of about 800 nm, the particle sizes range from 50 to 70 nm according to the corresponding SEM image (see Figure S1 in the Supporting Information), which is larger than that of the PbSe Bohr radius. Thus, it is reasonable that the band gap of the as-prepared larger PbSe hollow spheres exhibits no obvious size effect.

This facile one-pot synthetic route can be easily extended to the fabrication of the $NiSe_2$ hollow spheres. Figure 6 gives the XRD patterns of the $NiSe_2$ products obtained with different amounts of PVP at 150 °C, which matches well with the cubic phase $NiSe_2$ according to the JCPDS Card 41-1495. The size and morphology of the as-prepared $NiSe_2$ products obtained with 0.6 g PVP are consistent with that of the obtained PbSe hollow spheres in similar conditions. As indicated by both SEM and TEM images in Figure 7, the diameters of the obtained $NiSe_2$ are about 150 nm. In addition, the higher contrast along the edges of the spheres shown in Figure 7B reveals the hollow structure of the products. However, it is noted that the thickness of the $NiSe_2$ hollow spheres is much larger than that of the as-synthesized PbSe products. As estimated by the TEM images, the thickness of the $NiSe_2$ hollow spheres with diameters of about 150 nm is 50−60 nm (20−30 nm for PbSe hollow spheres with diameters of about 150−180 nm). Also for this reason, the hollow feature of the $NiSe_2$ spheres with diameters of about 800 nm obtained without the addition of the PVP cannot be observed through either SEM or TEM characterization, as shown in Figure 8, possibly due to the large thickness of the shells. In this situation, we could provide only indirect evidence for the hollow character of the $NiSe_2$ microspheres. To achieve this object, we dispersed the $NiSe_2$ hollow spheres with diameters of about 800 nm into the

(15) (a) Alivisatos, A. P. *Science* **1996**, *271*, 933. (b) Alivisatos, A. P. *Acc. Chem. Res.* **1999**, *32*, 387.
(16) (a) Du, H.; Chen, C. L.; Krishnan, R.; Krauss, T. D.; Harbold, J. M.; Wise, F. W.; Thomas, M. G.; Silcox, J. *Nano Lett.* **2002**, *2*, 1321. (b) Tan, T. T.; Selvan, S. T.; Zhao, L.; Gao, S. J.; Ying, J. Y. *Chem. Mater.* **2007**, *19*, 3112. (c) Harbold, J. M.; Wise, F. W. *Phys. Rev. B* **2007**, *76*, 125304. (d) Moreels, I.; Lambert, K.; De Muynck, D.; Vanhaecke, F.; Poelman, D.; Martins, J. C.; Allan, G.; Hens, Z. *Chem. Mater.* **2007**, *19*, 6101.
(17) (d) Evans, C. M.; Guo, L.; Peterson, J. J.; Maccagnano-Zacher, S.; Krauss, T. D. *Nano Lett.* **2008**, *8*, 2896.
(18) (a) Gorer, S.; Hodes, G. *J. Phys. Chem.* **1994**, *98*, 5338. (b) Gorer, S.; Yaron, A. A.; Hodes, G. *J. Phys. Chem.* **1995**, *99*, 16442.
(19) (a) Leslie-Pelecky, D. L.; Rieke, R. D. *Chem. Mater.* **1996**, *8*, 1770. (b) Zeng, H.; Sun, S. H. *Adv. Funct. Mater.* **2008**, *18*, 391. (c) Zhang, T.; Zhou, T. F.; Qian, T.; Li, X. G. *Phys. Rev. B* **2007**, *76*, 174415.

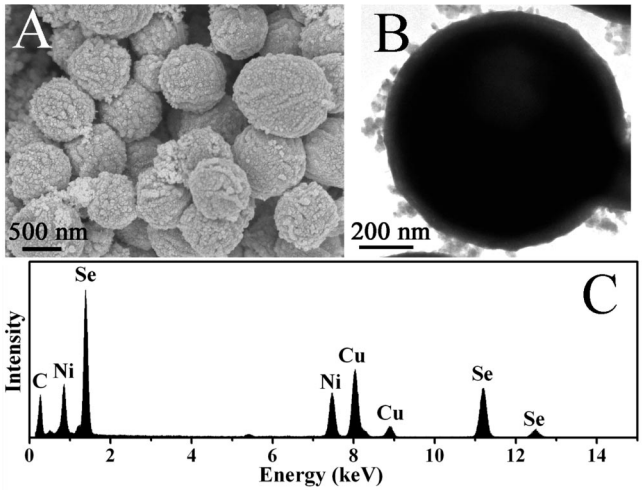

Figure 8. Morphology and composition analysis of the $NiSe_2$ hollow spheres obtained at 150 °C for 20 min without PVP: (A) typical SEM image, (B) TEM image, and (C) EDS spectrum.

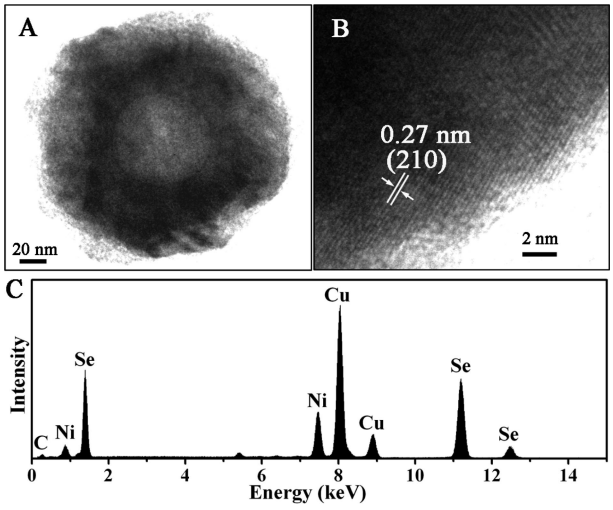

Figure 9. HRTEM and composition characterization of the $NiSe_2$ hollow spheres obtained at 150 °C for 20 min with 0.6 g of PVP: (A) TEM image of a randomly selected individual $NiSe_2$ hollow sphere, (B) typical lattice fringes, and (C) EDS spectrum taken from the sphere in (A).

ethanol and dealt with ultrasonic vibration for about 1 h. Very few of them are broken and they exhibit hollow character (see Figure S2 in the Supporting Information). The EDS analysis shown in Figure 8C, together with the XRD result (Figure 6A), confirms the formation of the cubic phase $NiSe_2$ products with an approximate molar ratio of 1:2.

The microstructure and composition analyses of $NiSe_2$ hollow spheres with diameters of about 150 nm are performed by HRTEM and EDS analyses, as shown in Figure 9. The HRTEM image (Figure 9B) taken from the individual hollow sphere shown in Figure 9A indicates that the lattice spacing is about 0.27 nm, whose value is quiet close to that of the cubic $NiSe_2$ (210) planes (0.268 nm from the JCPDS Card 41-1495). The EDS spectrum shown in Figure 9C gives that the approximate molar ratio of the Ni and Se is about 1:2, which is consistent with the XRD and HRTEM results.

It has been broadly reported that the magnetic nanomaterials exhibit unique and interesting magnetic properties due to both size and shape effects.[15] To investigate the magnetic properties of the as-prepared $NiSe_2$ hollow spheres with

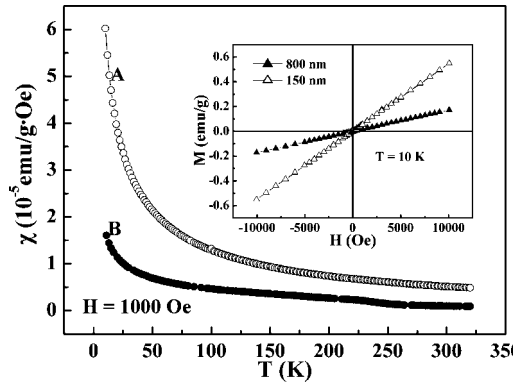

Figure 10. Temperature dependencies of magnetic susceptibility of the $NiSe_2$ hollow spheres with different diameters: (A) 150 nm and (B) 800 nm under the zero-field-cooled (ZFC) case. The inset is the corresponding magnetization loops measured at 10 K.

different diameters, the temperature dependencies of magnetization ($M-T$) were measured from 10 to 320 K, as shown in Figure 10. The magnetic susceptibility of the $NiSe_2$ hollow spheres with diameters of about 150 nm is about 5.28×10^{-6} emu/(g Oe) at 300 K, which is about five times larger than that of the $NiSe_2$ bulk counterpart,[20] whereas that of the $NiSe_2$ hollow spheres with diameters of about 800 nm is about 0.98×10^{-6} emu/(g Oe), which is close to the value of the $NiSe_2$ bulk counterpart.[20] As can be seen from the magnetization loops measured at 10 K (see the inset in Figure 10), no magnetic hysteresis loops are observed, which further confirms the paramagnetic feature of the $NiSe_2$ hollow spheres with different diameters.

To understand the shape evolution from solid Se spheres to metal selenides hollow spheres, we first ruled out the possibility of the galvanic replacement reaction mechanism through the observation of time-dependent products at 20 °C (see Figure S3 in the Supporting Information). It can be clearly seen that no hollow structure of the PbSe or $NiSe_2$ is obtained. Whereas, it should be noted that the XRD patterns (see Figure S4 in the Supporting Information) indicate that the products obtained with $Pb(CH_3COO)_2 \cdot 3H_2O$ and SeO_2 as precursors contain PbSe cubic phase while those obtained with $NiCl_2 \cdot 6H_2O$ and SeO_2 as precursors contain no obvious crystallized phase. The results demonstrate that the galvanic replacement between Pb^{2+} and Se could happen although no hollow structure could be formed through this reaction process, whereas that between Ni^{2+} and Se did not happen under the conditions involved in our work. Therefore, the hollow structure should be derived from other formation mechanisms. We carefully observed the morphologies of the time-dependent products during the formation of the PbSe and $NiSe_2$ hollow spheres at 150 °C, which may provide an important clew to disclose the growth mechanism. Typical TEM images were shown in Figure 11 for PbSe. According to these TEM images, of the intermediate products during the formation of hollow spheres, the growth process is schematically illustrated as shown in Figure 12, and the possible reaction procedures can be described as below: First,

(20) (a) Ogawa, S. *J. Appl. Phys.* **1979**, *50*, 2308. (b) Inoue, N.; Yasuoka, H.; Ogawa, S. *J. Phys. Soc. Jpn.* **1980**, *48*, 850. (c) Waki, S.; Kasai, N.; Ogawa, S. *Solid State Commun.* **1982**, *41*, 835.

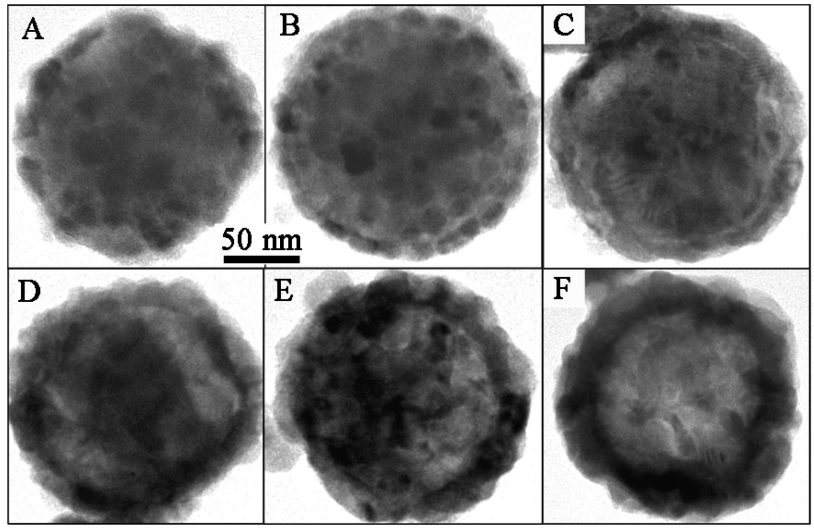

Figure 11. TEM images of the time-dependent products during the synthesis of PbSe hollow spheres obtained with 0.6 g of PVP (A) as soon as the temperature reaches 150 °C, (B) reaction for 2, (C) 3, (D) 5, (E) 7, and (F) 10 min at 150 °C.

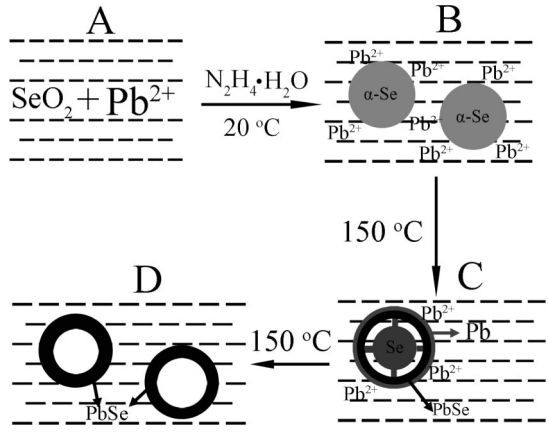

Figure 12. Schematic illustration of the involved formation process for the PbSe and $NiSe_2$ hollow spheres.

the dissolved SeO_2 in ethylene glycol can be easily transformed to brick red α-Se spheres by reducing SeO_2 with $N_2H_4 \cdot H_2O$ at about 20 °C, whereas the Pb^{2+} or Ni^{2+} cannot be reduced to Pb or Ni atoms at this stage (illustrations A and B in Figure 12). Subsequently, when the temperature increases to 150 °C, the generated Pb or Ni atoms obtained from the reduction of Pb^{2+} or Ni^{2+} by $N_2H_4 \cdot H_2O$ will randomly attach to the surface of the crystallized Se spheres, corresponding to the morphologies shown in images A and B in Figure 11. The corresponding EDS analysis (Figure S5A, Supporting Information) indicates that the atomic ratio of Pb and Se for the products is about 17:83. When the reaction time further increases to about 3 min after being heated to 150 °C, a core/shell structure with a little void between them is formed (Figure 11C). The mutual diffusion process could be continued through the bridge structure[3] and the void becomes larger with increasing reaction time, as indicated in images D and E in Figure 11 and schematically illustrated in Figure 12C. For the intermediate products after reaction at 150 °C for 7 min (Figure 11E), the atomic ratio of Pb and Se is increased to about 35:65, as shown in Figure S5B in the Supporting Information. The core material ultimately disappears and the hollow PbSe forms when the reaction time reaches 10 min, as shown in Figure 11F. This evolution process provides strong evidence that the Kirkendall effect could be the involved growth mechanism for the formation of PbSe and $NiSe_2$ hollow spheres in our work, which is similar to formation process in the previous literatures, such as the formation of the CoS_x and CoO hollow nanocrystals.[3,5] Similar evolution process can also be observed from the time-dependent products during the formation of $NiSe_2$ hollow spheres (Figures S6 and S7 in the Supporting Information), which further supports the Kirkendall effect formation mechanism in this work.

4. Conclusion

In summary, PbSe and $NiSe_2$ hollow spheres with controllable diameters were successfully obtained by a two-stage temperature-controlled, solution-phase method. Time-dependent products demonstrate that the involved mechanism for the hollow sphere formation could be the Kirkendall effect process. The optical property of the PbSe and the magnetic property of the $NiSe_2$ were investigated and the results indicate that both the optical and magnetic properties exhibit notable size dependence. This method provides a simple one-pot route for synthesizing metal selenides hollow structures and could be extended to other material systems.

Acknowledgment. This work was supported by the National Natural Science Foundation of China (50721061, 50832007 and 50772111) and the National Basic Research Program of China (2006CB922005 and 2006CB929502).

Supporting Information Available: Additional SEM and TEM images, XRD patterns, and EDS spectra (PDF). This material is available free of charge via the Internet at http://pubs.acs.org.

CM803307F